Biosynthesis MgO and ZnO nanoparticles using chitosan extracted from Pimelia Payraudi Latreille for antibacterial applications

Ilham Ben Amor
University of El Oued
Hadia Hemmami
University of El Oued
Salah Eddine Laouini
University of El Oued
Hachemi Ben Temam
Université Mohamed Khider
Hamza Zaoui
Laboratoire de Physique des Couches Minces et Applications, Université Mohamed Khider
Ahmed Barhoum (ahmed.barhoum@dcu.ie)
Dublin City University

Research Article

Keywords: Biopolymer, biological synthesis, Chitosan extraction, antimicrobial nanoparticles, antibacterial activity

Posted Date: September 14th, 2022

DOI: https://doi.org/10.21203/rs.3.rs-2053261/v1

Abstract

Chitosan (CS) is one of the most abundant biopolymers in nature, with superior properties including biocompatibility, biodegradability, lack of toxicity, antimicrobial activity, acceleration of wound healing, and stimulation of the immune system. In this study, chitosan was extracted from the exoskeletons of the beetle (Pimelia Payraudi Latreille) and then used for the biosynthesis of MgO NPs and ZnO NPs. The extracted chitosan exhibited excellent physicochemical properties, including high extraction yield (39%), high degree of deacetylation (90%), low ash content (1%), high fat-binding capacity (366%), and odd crystallinity index (51%). The MgO NPs and ZnO NPs exhibited spherical morphology with crystallite sizes of 17 nm and 29 nm, particle sizes of about 20-70 nm and 30-60 nm, and bandgap energy of 4.43 and 3.34 eV, respectively. Antibacterial assays showed that the extracted chitosan showed high antibacterial activity against Gram-(+/-) bacteria, while ZnO NPs showed much stronger antibacterial activity against Gram-(+) bacteria than against Gram(-) bacteria. For MgO NPs, the antibacterial activity against Gram-(+) bacteria was lower than that against Gram-(-) bacteria. The results suggest that the synthesized MgO NPs and ZnO NPs are excellent antibacterial agents for therapeutic applications.

1. Introduction

Antimicrobial nanoparticles are potential broad-spectrum antibiotics that can overcome resistance to conventional antibiotics[1]. Adhesion of nanoparticles to microbial cells and reactive oxygen species and their penetration into cells have been identified as the main antimicrobial mechanisms of action [2]. Depending on particle size, capping technique, and concentration, nanoparticles can be either bactericidal or bacteriostatic [3]. In addition, the development of resistance to nanoparticles is less likely, but not impossible. Physicochemical approaches such as sol-gel and solvothermal methods are the most common methods for preparing metals and metal oxide nanoparticles [4]. However, these methods are usually expensive and can pollute the environment. Therefore, an alternative green biosynthesis method was used to synthesize nanoparticles. Plant extracts or biopolymer molecules can be used as reducing agents to produce nanoparticles [5, 6]. The biosynthesis methods using plant extracts or biopolymer molecules are very important in the preparation of Ag, Au, Cu, ZnO, and MgO NPs [7, 8]

Chitosan, a natural polycationic polymer, has been used as a reducing agent for nanoparticle synthesis and an antimicrobial agent for biomedical applications. Chitosan composites with nanoparticles have significant antibacterial activity against a variety of bacterial pathogens. Chitosan is found mainly in the exoskeletons of arthropods, in Saccharomyces cerevisiae, and in the cell walls of fungi [9]. Chitosan is found in the cuticle of insects and crustaceans, which contains 15–20% chitin along with proteins, minerals, and pigments [7]. Chitosan is commercially produced by deacetylation of the chitin extracted from the exoskeleton of crustaceans. The degree of deacetylation ranges from 60–100% for commercial chitosans. During extraction, the proteins, minerals, and pigments of the cuticle are separated from the chitin matrix using chemicals under mild conditions. Commercially produced chitosan has an average Mwt of 4000-20,000 Daltons and a pKa of ~ 6.5 [10]. The amino groups make chitosan water-soluble and

bind readily to negatively charged functional groups. Chitosan is a non-toxic, biocompatible, and biodegradable biopolymer with antitumor, antioxidant, and antimicrobial properties [11].

Chitosan is gaining importance as biopolymers used as reducing agents, shapers, or size adjusters in the production of metal and metal oxide nanoparticles [12]. Coating the surfaces of nanoparticles with chitosan makes them more biocompatible with normal cells. Chitosan has been shown to regulate drug release, promote mucosal adhesion and tissue penetration [13], support cell interaction [14], and enhance antimicrobial activity [15]. The amino groups of chitosan are rapidly protonated in the acidic state and can combine with anionic functional groups. Large amounts of amino groups on chitosan lead to easy binding of metal oxide nanoparticles with many bioactive molecules, including drugs, enzymes, protons, etc [16]. Chitosan-coated nanoparticles possess antibacterial and antioxidant activity, as well as antituberculosis activity and antifungal activity against Candida [17]. The antibacterial activity of chitosan is due to its electric charge and high adsorption capacity, as well as chemical processes that enable them to effectively destroy the bacterial cell membrane and inhibit the growth of bacterial cells [18].

Given the growing concern about biofilm-associated infections and drug-resistant bacteria, the development of new antibacterial agents is a pressing concern [19, 20]. The present work aims to isolate chitosan from beetle (Pimelia Payraudi Latreille) and then use the extracted chitosan to prepare MgO NPs and ZnO NPs. Various physical characterization methods such as extraction yield, deacetylation degree (DD), ash content (AC), moisture content measurement (MC), water binding capacity (WBC), and fat binding capacity (FBC) were performed for the synthesized chitosan. Chitosan, ZnO NPs, and MgO NPs were characterized by UV-Vis, FTIR, XRD, and SEM. The antibacterial activity of chitosan, MgO NPs, and ZnO NPs was evaluated against Staphylococcus Aureus (ATCC6538), Bacillus Subtiliis (ATCC6633), Listeria Innocua (CLIP74915), Pseudomonas Aeruginosa (ATCC9027) and Salmonella Typhimuruim (ATCC14028). Chitosan is enriched with amino functional groups which bind with ZnO NPs and MgO NPs, improving their properties and preventing nanoparticle agglomeration. Therefore, we believe that the prepared chitosan, ZnO NPs, and MgO NPs could be used as antimicrobial nanomaterials in the cosmetics, biomedical, and pharmaceutical industries.

2. Materials And Methods

2.1. Materials

Zinc chloride ($ZnCl_2$, 99%), magnesium chloride hydrates ($MgCl_2$,$6H_2O$, 98%), sodium hydroxide (NaOH, 97%), hydrochloric acid (HCl, 99%), acetic acid (CH COOH, 99.5%), hydrogen peroxide (H_2O_2, 98%), and dimethyl sulfoxide (DMSO, 99%) were purchased from Biochem Chemophara. Mueller-Hinton agar was purchased from Bioscan Industrie, Algeria. The beetles (Pimelia Payraudi Latreille) were the primary supplier for chitosan extraction. The Beetles were collected from different locations in Algeria and the exoskeleton was selected for chitosan extraction.

2.2. Extraction of chitosan

Beetles were starved in the laboratory for 3 days to remove the gut contents. Then, the beetles were washed with distilled water, dried, ground, and then stored at -20°C. As shown in Fig. 1, the exoskeleton of the beetles was thoroughly freed from loose tissue, cleaned, dried, and crushed to fit through a 250 µm mesh sieve [21]. Briefly, 30 g of the sample (beetle exoskeleton) was treated with 1 M HCl (demineralization) at a solid to liquid ratio of 1:15 for 1 hour at 40°C. After demineralization, the resulting solid fraction was rinsed with distilled water until the pH returned to pH = 7. The extracted chitin was deproteinization with 1 M NaOH at 80°C for 2 h. The chitin was then filtered, washed, and then decolorized by treatment with 10% H_2O_2 at 50°C for 30 min. The chitin was then neutralized by rinsing with distilled water until pH = 7 was reached. The decolorized chitin was subjected to a deacetylation procedure in which it was treated with 50 wt% NaOH at 100°C for 4 hours. The precipitate was washed with distilled water and the resulting chitosan was dried under vacuum at 50°C for 24 hours.

2.3. Biosynthesis of MgO NPs and ZnO NPs

To prepare MgO NPs and ZnO NPs from the chitosan extract, a solution with a concentration of 1% w/v chitosan in an acetic acid solution was prepared. After completion of the dissolution process, 5 ml of the previously prepared chitosan was mixed with 50 ml of an aqueous solution containing $MgCl_2.6H_2O$ or $ZnCl_2$ at a concentration of 0.1 M for 4 h. The pH of each mixture was adjusted by adding 0.1 M NaOH with constant stirring until the pH became basic (pH = 9), at 60°C. The precipitate was then rinsed several times with deionized water, centrifuged at a speed of 2500 rpm, and then heated at 500°C for 4 hours to remove all organic residues.

2.4. Physicochemical characterization

After drying the chitosan extract, the dried chitosan was weighed and the chitosan content was calculated as follows: Yield (%)=(weight of chitosan, g)/(weight of beetle exoskeleton, g)×100 [22]. The ash content of chitosan was determined gravimetrically by combustion in an air atmosphere using a constant weight crucible at 550°C for 3 h.The degree of deacetylation (DD) of chitosan was determined by FTIR spectroscopy using the following equation: DD (%) = 100 - [100*(A_{1655}/A_{3450})/1.33] .Where: A_{3450} and A_{1655} are the heights of the absorption bands of the hydroxyl and amide groups, respectively. The factor of 1.33 indicates the value of the A_{1655}/A_{3450} ratio for fully N-acetylated chitosan [23]. The ash content of chitosan was determined according to the method of R.H. Rødde et al. (2008). The following equation was used to determine the ash content: Ash % = (W_2 / W_1) x 100, where W_1 and W_2 are the initial weight of the chitosan sample and the weight of the residue (grams), respectively. The moisture content of the prepared chitosan was determined gravimetrically by vacuum drying at 110°C for 24 hours. The moisture content (MC, %) = (W_1-W_2/ W_1) x 100, where W_1 and W_2 are the weights of the wet and oven-dried samples, respectively [24]. Water binding capacity (WBC) and fat binding capacity (FBC) were determined according to a modified method by Wang and Kinsella [25]. Briefly, a centrifuge tube containing 0.5 g of chitosan was weighed first. Then, 10 mL of water for the WBC test and soybean oil for

the FBC test were added to the chitosan and mixed in the centrifuge tube for 1 min using a vortexer. The mixture was allowed to stand at 25°C for 30 min, shaken every 10 min for 5 seconds, and centrifuged at 3200 rpm for 25 min. After decanting the supernatant, the tube was reweighed. WBC and FBC were calculated as follows: WBC% = (water-bound, g / initial weight chitosan, g) x 100 and FBC% = (fat-bound, g / initial weight chitosan, g) x 100 [26].

The crystalline structure of chitosan, MgO NPs, and ZnO NPs were studied by using X-ray diffraction (XRD, Rigaku Miniflex 600). A UV-Vis spectrophotometer (Jasco V160 UV-Vis) was used to record the absorption spectra of chitosan, MgO NPs, and ZnO NPs. The UV-Vis spectra of ZnO NPs and MgO NPs were studied by dispersing 0.1 mg each of ZnO NPs and MgO NPs in 2 ml of distilled water. The optical properties of chitosan were investigated by dissolving 0.1 mg of chitosan in 2 ml of acetic acid. The band gap energy (Eg) was estimated using the Tauc relationship $(\alpha h\nu) = A (h\nu - Eg)^n$ [27]. Here α is the absorption coefficient, h is Planck's constant, A is a constant, Eg is the energy bandgap, and n is a constant equal to ½ for the direct band gap [28]. The IR spectra were characterized using a Nicolet iS50 FT-IR spectrometer with the KBr technique [29]. Particle size, morphology, and elemental composition were studied with a scanning electron microscope (FESEM, Leo Supra 55-Zeiss Inc., Germany).

2.5. Antibacterial bioassay

Agar well diffusion method was used to test the antibacterial activity of chitosan, MgO NPs, and ZnO NPs against a variety of bacterial strains, particularly Staphylococcus Aureus (ATCC6538), Bacillus Subtiliis (ATCC6633), Listeria Innocua (CLIP74915), Pseudomonas Aeruginosa (ATCC9027), and Salmonella Typhimuruim (ATCC14028). Culture plates are prepared and streaked with 100 µl of a 24 h matured broth culture of bacterial strains using a sterile glass rod. Wells are made with a sterile cork borer; 6-mm wells are made in each Petri plate. Different concentrations of MgO NPs and ZnO NPs (2 mg/mL, 4 mg/mL, 6 mg/mL in DMSO) and chitosan (1%, 4%, and 8% in acetic acid) were used to study antibacterial activity. The antibacterial assay of the samples tested against ciprofloxacin (CIP-5) as reference. The plates were incubated for 24 h at 37°C. The diameters of the zone of inhibition after the incubation period are summarized in Table 1.

3. Results And Discussion

3.1. Characteristics of chitosan

Chitosan is a deacetylated derivative of chitin, both are biocompatible, biodegradable, and non-toxic. Previous studies reported that the yield of chitosan from other insects was 2 to 79% [30]. This study showed a chitosan yield of 39%. The lower limit of yield (39%) of chitosan is due to the removal of the proteins and impurities during the deacetylation and precipitation process. In contrast to chitin, chitosan has a large proportion of a highly protonated free amino group that tends to bind with metal and metal oxide nanoparticles. A DD of 70–85% is the average DDA of chitosan, which can be partially dissolved in water [31]. The DD value of the extracted chitosan was calculated by the FTIR analysis and was 90%.

This high DD of value allows chitosan to be readily dissolved in water. Reducing the molecular weight of chitosan by degradation is beneficial for increasing its water solubility. Chitosan with DD value of ≤ 80% is usually recommended for nucleic acid delivery applications [32]. The ash content of chitosan isolated from beetles was 1%. Chitosan without demineralization had high ash content which may reach up to 39%. The appearance of chitosan without demineralization is white and chalky, while the other chitosan is creamy white. Chitosan is naturally hygroscopic, so commercial chitosan may be affected by moisture absorption during storage. The MC of chitosan isolated from the beetle was 9%. The WBC and FBC of commercial chitosan are 458–805% and 310–530%, respectively [26] .The WBC and FBC of the extracted chitosan isolated from beetles are 577% and 366%, respectively.

Table 1
Characteristics of the chitosan extract.

Characteristics of the Chitosan	Value
Extraction Yield (Y)	39%
Degree of Deacetylation (DD)	90%
Ash contents (AC)	1%
Moisture content (MC)	9%
Water binding capacity (WBC)	577%
Fat binding capacity (FBC)	366%
Crystallinity index (CI)	51%

3.2. UV-vis spectroscopy

Figure 3 shows the UV-vis absorption spectra of chitosan, ZnO NPs, and MgO NPs. The chitosan has two main absorbance bands, a weak peak at 270 nm and a strong peak at 220 nm. The band at 270 nm is due to the n-π* transition of the amino groups. The spectral absorption at 320 nm is due to the n-π* transition for the carboxyl or carbonyl groups [23]. The UV-vis spectra of the MgO and ZnO NPs show characteristic absorption bands at 218 nm and 321 nm, respectively. The bandgap energy of MgO NPs and ZnO NPs was estimated by plotting $(\alpha h\nu)^2$ versus energy (eV), as shown in Fig. 3b. The bandgap energies of MgO NPs and ZnO NPs are found to be 4.4 and 3.34 eV, respectively. The sharp UV bands shown for MgO NPs and ZnO NPs in the UV range prove the narrow nanosize distribution of these nanoparticles and their potential applications in sunscreens or antiseptic ointments.

3.3. FTIR spectroscopy

FTIR spectra of chitosan showed a broader band at 3100–3500 cm^{-1} corresponding to the -OH and the -NH stretching vibrations [33]. The bands at 2862 cm^{-1} correspond to the stretching of polysaccharide bonds CH. The band at 1650 cm^{-1} is attributed to amide I resulting from the removal of the acetyl group

(deacetylated chitin) [34]. The band at 1580 cm^{-1} corresponds to an amide II (-NH2 bending). The degree of acetylation of the chitosan extract was calculated from the FTIR spectra and was found to be 90% (Table 1). In the case of MgO, the broadband at about 433–769 cm^{-1} is attributable to the metal-oxygen bending vibration. A broad band at about 3461 cm^{-1} is attributed to the stretching frequency of H-O-H. The Mg-O stretching vibration corresponds to the broad band stretching vibration at about 673 cm^{-1} [35]. The bending deformation vibrations of ZnO NPs can be seen from the peaks at 1636 cm^{-1}. The strong vibrational bands at 445 cm^{-1} are assigned to the stretching modes for the formation of ZnO NPs [36].

3.4. X-ray diffraction

Crystallininity and crystalline structure of chitosan strongly depend on degree of deacetylation of chitin. The XRD pattern of chitosan shows three diffraction peaks occurring at 10.4°, 20.0°, and 30°, corresponding to the (020), (110), and (100) planes of the crystal lattice, respectively. The intensity of the peak at 10.4° is lower than that at 20.0°. This is due to the intramolecular hydrogen bonds formed after deacetylation [37]. The crystallinity of chitosan was determined using the following equation: Crystallinity index=$(I_{110}-I_{am})/I_{110}$. Where I_{am} is the intensity of amorphous diffraction centered at 2θ = 10° and I_{110} is the maximum diffraction intensity at centered 2θ = 20° [33, 38]. The determined value of the crystallinity index is 51%. Figure 4b shows the XRD pattern of a sample of MgO NPs and ZnO NPs. In the case of MgO NPs, the peaks at 2θ = 36.85°, 42.79°, 62.19°, 74.59°, and 78.58° correspond to (111), (200), (220), (311), and (222), respectively. This is inconsistent with the JCPDS No. 01-089-7746 map of MgO [39].The peaks of ZnO NPs at 2θ = 31.9°, 34.6°, 36.4°, 47.76°, 56.7°, 63.0°, 66.5°, 68.1°, 69.2°, 72.8°, and 77.9° correspond to (100), (002), (101), (102), (110), (103), (200), (112), (201), (004), and (202), respectively [40].This is inconsistent with the JCPDS card (00-036-1451) of ZnO. The crystallite size of MgO NPs and ZnO NPs was calculated using the Debye-Scherer equation: D = Kλ/(β-cosθ) [41]. Where d is the average crystallite size, λ is the wavelength of X-ray (0.15406 nm), K is a constant assumed to be 0.9, and β is the FWHM of the intensity for the peak centered at 20°; and θ is the Bragg angle. The average crystallite size of the MgO NPs is 17 nm, while the crystallite size of the ZnO NPs is 29 nm.

3.5. Scanning Electron Microscopy

SEM was used to analyze the morphology of the extracted chitosan, ZnO NPs, and MgO NPs. Chitosan extracted from Pimelia Payraudi Latreille has a fibrous structure with a rough surface similar to the structure of shrimp and crab. The morphology and particle size of ZnO NPs and MgO NPs are affected by several factors, such as salt concentration, chitosan concentration, solution pH, and temperature [42].SEM images show that the ZnO and MgO NPs have an average particle size of about 45 nm with spherical morphology. SEM-EDS elemental analysis shows that Mg and O were present in the MgO NPs at atomic percentages of 47.7% and 48.5%, respectively. The atomic mass compositions of Zn and O in the ZnO NPs were 37.5% and 62.6%, respectively. The SEM-EDX analysis confirmed the formation of MgO NPs and ZnO NPs.

3.6. Antibacterial activities

Figure 7 shows the antibacterial activity of chitosan, MgO NPs, and ZnO NPs against the Gram-(+) bacteria (Staphylococcus Aureus, Bacillus Subtiliis, Listeria Innocua) and Gram-(-) bacteria (Pseudomonas Aeruginosa, Salmonella Typhimuruim). Figure 7a shows that the zone of inhibition of chitosan increases with increasing chitosan concentration. The main factors affecting the antibacterial activity of chitosan include the type of bacteria, growth phase, chitosan concentration, chitosan Mwt, solution pH, and temperature [43]. Chitosan is most active on the surface of bacterial cells and leads to permeabilization of the bacterial membrane mainly by electrostatic interaction. The positive charge of the protonated amino group of chitosan interacts with the negatively charged molecules on the bacterial cell membrane and eventually leads to bacterial cell death [43, 44]. Silva et al [45] used Buriti oil in chitosan films and observed a complete barrier against microorganisms. Devlieghere et al [46] quantified the antimicrobial activity of commercial chitosan with a high degree of deacetylation (94%) and low Mwt on various spoilage pathogens. The authors noted that Gram(-) bacteria were very sensitive to the chitosan used, while the sensitivity of Gram(+) bacteria was very different.

Figure 7b shows the strong antibacterial activity of MgO NPs against Gram(-) bacteria (Salmonella Typhimurium), but shows no significant effect on Gram(+) bacteria. The mechanism of action of MgO NPs with bacterial cells depends on the cell wall structure and the binding sites of MgO NPs to the cell surface, subsequently the interaction of Mg NPs with internal cell components. In contrast to MgO NPs, ZnO NPs have a much stronger antibacterial effect on Gram-(+) bacteria compared to Gram-(-) bacteria (Fig. 7c). The difference between Gram-(-) bacteria and Gram-(-) bacteria in the outer membrane is probably the main reason for this behavior [47]. The cell wall of Gram-(-)-bacteria consists of two cell membranes, an outer membrane and a plasma membrane with a thin peptidoglycan layer. On the opposite side, the MgO NPs and ZnO NPs have also different crystal structure, and surface charges, which interacts differently with Gram-(+) bacteria and with Gram-(+) bacteria [48].

Conclusion

Chitosan was extracted from the exoskeletons of the beetle (Pimelia Payraudi Latreille) and then used for the biosynthesis of antibacterial MgO NPs and ZnO NPs. After precipitation, the yield of pure chitosan from the beetle Pimelia Payraudi Latreille was 39%. The extracted chitosan exhibited excellent physicochemical properties compared to previously published studies: Extraction yield (39%), deacetylation degree (90%), ash content (1%), moisture content (9%), water binding capacity (577%), fat binding capacity (366%), crystallinity index (51%). The ZnO NPs and MgO NPs prepared from chitosan exhibited a spherical morphology with an average particle size of about 45 and a crystallite of 25 nm. The antibacterial properties of chitosan, MgO NPs, and ZnO NPs were investigated against different types of Gram-(-) and Gram-(+) bacteria by the agar well diffusion method. Chitosan showed good antibacterial activity against both Gram-(+) and Gram-(-) bacteria. The ZnO NPs showed much stronger antibacterial activity against Gram-(+) bacteria than against Gram-(-) bacteria. While the MgO NPs showed strong antibacterial activity against Gram-(-) bacteria and low activity against Gram-(+) bacteria. The results

suggest that the chitosan extracted from the exoskeletons of the beetle and the biosynthesized MgO NPs and ZnO NPs are excellent antibacterial agents for biomedical applications.

Declarations

Conflict of Interest

No relevant financial or non-financial interests were held by the authors.

Acknowledgments

Ahmed Barhoum would like to thank the Joint Egyptian Japanese Scientific Cooperation (JEJSC, ID 42811), and the Irish Research Council (GOIPD/2020/340) for financial support. Open Access funding is provided by the IReL Consortium, thanks to Dublin City University (DCU) along with the Irish Research eLibrary (IReL) for providing an open access publishing agreement with a springer nature. We are grateful to the various contributors who supplied samples and/or measurements for this study: Djamila Berra and Ali Tliba.

References

1. Laouini SE, Bouafia A, Soldatov AV, Algarni H, Tedjani ML, Ali GA, et al (2021) "Green synthesized of Ag/Ag2O nanoparticles using aqueous leaves extracts of Phoenix dactylifera L. and their azo dye photodegradation," *Membranes*, vol. 11, p. 468,
2. Barhoum A, García-Betancourt ML, Jeevanandam J, Hussien EA, Mekkawy SA, Mostafa M, et al (2022) "Review on natural, incidental, bioinspired, and engineered nanomaterials: history, definitions, classifications, synthesis, properties, market, toxicities, risks, and regulations," *Nanomaterials*, vol. 12, p. 177,
3. Harish V, Tewari D, Gaur M, Yadav AB, Swaroop S, Bechelany M, et al (2022) "Review on nanoparticles and nanostructured materials: Bioimaging, biosensing, drug delivery, tissue engineering, antimicrobial, and agro-food applications," *Nanomaterials*, vol. 12, p. 457,
4. Salama A, Abouzeid R, Leong WS, Jeevanandam J, Samyn P, Dufresne A, et al (2021) "Nanocellulose-based materials for water treatment: adsorption, photocatalytic degradation, disinfection, antifouling, and nanofiltration," *Nanomaterials*, vol. 11, p. 3008,
5. Belaiche Y, Khelef A, Laouini SE, Bouafia A, Tedjani ML, Barhoum A (2021) Green synthesis and characterization of silver/silver oxide nanoparticles using aqueous leaves extract of Artemisia herba-alba as reducing and capping agents,. Rev Rom Mater 51:342–352
6. Hamimed S, Abdeljelil N, Landoulsi A, Chatti A, Aljabali AA, Barhoum A (2022) "Bacterial cellulose nanofibers: biosynthesis, unique properties, modification, and emerging applications," *Handbook of Nanocelluloses: Classification, Properties, Fabrication, and Emerging Applications*, pp. 1–38,

7. Said MM, Rehan M, El-Sheikh SM, Zahran MK, Abdel-Aziz MS, Bechelany M, et al (2021) "Multifunctional hydroxyapatite/silver nanoparticles/cotton gauze for antimicrobial and biomedical applications," *Nanomaterials*, vol. 11, p. 429,
8. Djamila B, Eddine LS, Abderrhmane B, Nassiba A, Barhoum A (2022) "In vitro antioxidant activities of copper mixed oxide (CuO/Cu2O) nanoparticles produced from the leaves of Phoenix dactylifera L,"Biomass Conversion and Biorefinery, pp.1–14,
9. Iber BT, Kasan NA, Torsabo D, Omuwa JW (2022) A review of various sources of chitin and chitosan in nature,. J Renew Mater 10:1097
10. Rinaudo M (2006) Chitin and chitosan: Properties and applications,. Prog Polym Sci 31:603–632
11. Jiménez-Gómez CP, Cecilia JA (2020) "Chitosan: a natural biopolymer with a wide and varied range of applications," *Molecules*, vol. 25, p. 3981,
12. Ottonelli M, Zappia S, Demartini A, Alloisio M (2020) "Chitosan-stabilized noble metal nanoparticles: study of their shape evolution and post-functionalization properties," *Nanomaterials*, vol. 10, p. 224,
13. Ahmed TA, Aljaeid BM (2016) "Preparation, characterization, and potential application of chitosan, chitosan derivatives, and chitosan metal nanoparticles in pharmaceutical drug delivery," *Drug design, development and therapy*, vol. 10, p. 483,
14. Zubareva A, Svirshchevskaya E (2016) Interactions of chitosan and its derivatives with cells,. Appl Biochem Microbiol 52:465–470
15. Phan TTV, Phan DT, Cao XT, Huynh T-C, Oh J (2021) "Roles of chitosan in green synthesis of metal nanoparticles for biomedical applications," *Nanomaterials*, vol. 11, p. 273,
16. Hojnik Podrepšek G, Knez Ž, Leitgeb M (1913) "Development of chitosan functionalized magnetic nanoparticles with bioactive compounds," *Nanomaterials*, vol. 10, p. 2020
17. Sharifiaghdam M, Shaabani E, Asghari F, Faridi-Majidi R (2022) "Chitosan coated metallic nanoparticles with stability, antioxidant, and antibacterial properties: Potential for wound healing application,". J Appl Polym Sci 139:51766
18. Yilmaz Atay H (2019) "Antibacterial activity of chitosan-based systems,". Functional chitosan. ed: Springer, pp 457–489
19. Youssef AM, Moustafa HA, Barhoum A, Hakim AEFAA, Dufresne A (2017) "Evaluation of the Morphological, Electrical and Antibacterial Properties of Polyaniline Nanocomposite Based on Zn/Al-Layered Double Hydroxides," *ChemistrySelect*, vol. 2, pp. 8553–8566,
20. Forster RJ, De Eguilaz MR, Barhoum A, Cumba LR (2022) "Electrochemical (Bio) Sensors for Bacteria and Biofilms,"
21. Kaya M, Seyyar O, Baran T, Turkes T (2014) Bat guano as new and attractive chitin and chitosan source,. Front Zool 11:1–10
22. Sanuja R, Kalutharage NK, Cumaranatunga PRT (2017) "Selection of the most suitable crustacean exoskeleton waste from fish processing industry to isolate chitosan,"Sri Lanka Journal of Aquatic Sciences, vol. 22,

23. Hao G, Hu Y, Shi L, Chen J, Cui A, Weng W et al (2021) Physicochemical characteristics of chitosan from swimming crab (Portunus trituberculatus) shells prepared by subcritical water pretreatment,. Sci Rep 11:1–9
24. Klute A (1986) "Water retention: laboratory methods," *Methods of soil analysis: part 1 physical and mineralogical methods*, vol. 5, pp. 635–662,
25. Samar MM, El-Kalyoubi M, Khalaf M, Abd El-Razik M (2013) "Physicochemical, functional, antioxidant and antibacterial properties of chitosan extracted from shrimp wastes by microwave technique,". Annals of Agricultural Sciences 58:33–41
26. Marei NH, Abd El-Samie E, Salah T, Saad GR, Elwahy AH (2016) Isolation and characterization of chitosan from different local insects in Egypt,. Int J Biol Macromol 82:871–877
27. Barhoum A, El-Maghrabi HH, Nada AA, Sayegh S, Roualdes S, Renard A et al (2021) Simultaneous hydrogen and oxygen evolution reactions using free-standing nitrogen-doped-carbon–Co/CoO x nanofiber electrodes decorated with palladium nanoparticles,. J Mater Chem A 9:17724–17739
28. Bouafia A, Laouini SE, Tedjani ML, Ali GA, Barhoum A (2021) "Green biosynthesis and physicochemical characterization of Fe3O4 nanoparticles using Punica granatum L. fruit peel extract for optoelectronic applications,"Textile Research Journal, p.00405175211006671,
29. Barhoum A, García-Betancourt ML (2018) "Physicochemical characterization of nanomaterials: Size, morphology, optical, magnetic, and electrical properties,". Emerging applications of nanoparticles and architecture nanostructures. ed: Elsevier, pp 279–304
30. Zainol Abidin NA, Kormin F, Zainol Abidin NA, Mohamed Anuar NAF, Abu Bakar MF (2020) The potential of insects as alternative sources of chitin: An overview on the chemical method of extraction from various sources,. Int J Mol Sci 21:4978
31. Pacheco-Torgal F, Ivanov V, Karak N, Jonkers H (2016) Biopolymers and biotech admixtures for eco-efficient construction materials. Woodhead Publishing
32. Aranda-Barradas ME, Trejo-López SE, Del Real A, Álvarez-Almazán S, Méndez-Albores A, García-Tovar CG et al (2022) Effect of molecular weight of chitosan on the physicochemical, morphological, and biological properties of polyplex nanoparticles intended for gene delivery,. Carbohydr Polym Technol Appl 4:100228
33. Kumirska J, Czerwicka M, Kaczyński Z, Bychowska A, Brzozowski K, Thöming J et al (2010) Application of spectroscopic methods for structural analysis of chitin and chitosan,. Mar Drugs 8:1567–1636
34. Ben Seghir B, Benhamza M (2017) "Preparation, optimization and characterization of chitosan polymer from shrimp shells,". J Food Meas Charact 11:1137–1147
35. Kandiban M, Vigneshwaran P, Potheher IV (2015) "Synthesis and characterization of mgo nanoparticles for photocatalytic applications," in *Department of Physics, Bharathidasan Institute of Technology (BIT) Campus, Anna University, Tiruchirappalli, Tamilnadu, India, Conference Paper*,
36. Handore K, Bhavsar S, Horne A, Chhattise P, Mohite K, Ambekar J et al (2014) "Novel green route of synthesis of ZnO nanoparticles by using natural biodegradable polymer and its application as a

catalyst for oxidation of aldehydes,". J Macromolecular Sci Part A 51:941–947

37. Kaya M, Baran T, Asan-Ozusaglam M, Cakmak YS, Tozak KO, Mol A et al (2015) Extraction and characterization of chitin and chitosan with antimicrobial and antioxidant activities from cosmopolitan Orthoptera species (Insecta),. Biotechnol Bioprocess Eng 20:168–179
38. Kaya M, Baran T, Erdoğan S, Menteş A, Özüsağlam MA, Çakmak YS (2014) Physicochemical comparison of chitin and chitosan obtained from larvae and adult Colorado potato beetle (Leptinotarsa decemlineata),. Mater Sci Engineering: C 45:72–81
39. El-Nahhal IM, Kodeh FS, Salem JK, Hammad T, Kuhn S, Hempelmann R, et al (2019) "Silica, mesoporous silica and its thiol functionalized silica coated MgO and Mg (OH) 2 materials," *Chemistry Africa*, vol. 2, pp. 267–276,
40. Farahmandjou M, Jurablu S (2014) Co-precipitation synthesis of zinc oxide (ZnO) nanoparticles by zinc nitrate precursor,. Int J Bio Inor Hybr Nanomater 3:84
41. El-Sheikh SM, Barhoum A, El-Sherbiny S, Morsy F, El-Midany AA-H, Rahier H (2019) Preparation of superhydrophobic nanocalcite crystals using Box–Behnken design,. Arab J Chem 12:1479–1486
42. Hassan SE-D, Fouda A, Saied E, Farag MM, Eid AM, Barghoth MG et al (2021) Rhizopus Oryzae-mediated green synthesis of magnesium oxide nanoparticles (MgO-NPs): A promising tool for antimicrobial, mosquitocidal action, and tanning effluent treatment,. J Fungi 7:372
43. Ardean C, Davidescu CM, Nemeş NS, Negrea A, Ciopec M, Duteanu N et al (2021) "Factors influencing the antibacterial activity of chitosan and chitosan modified by functionalization,". Int J Mol Sci 22:7449
44. Mendoza G, Regiel-Futyra A, Andreu V, Sebastian V, Kyzioł A, Stochel Gy et al (2017) "Bactericidal effect of gold–chitosan nanocomposites in coculture models of pathogenic bacteria and human macrophages,". ACS Appl Mater Interfaces 9:17693–17701
45. de Silva M, Lopes PS, da Silva CF, Yoshida CM (2016) "Active packaging material based on buriti oil–Mauritia flexuosa Lf (Arecaceae) incorporated into chitosan films,"Journal of Applied Polymer Science, vol. 133,
46. Devlieghere F, Vermeulen A, Debevere J (2004) "Chitosan: antimicrobial activity, interactions with food components and applicability as a coating on fruit and vegetables,". Food Microbiol 21:703–714
47. Tan KX, Barhoum A, Pan S, Danquah MK (2018) "Risks and toxicity of nanoparticles and nanostructured materials,". Emerging applications of nanoparticles and architecture nanostructures. ed: Elsevier, pp 121–139
48. Wang L, Hu C, Shao L (2017) The antimicrobial activity of nanoparticles: present situation and prospects for the future,. Int J Nanomed 12:1227
49. Li B, Wang X, Chen R, Huangfu W, Xie G (2008) Antibacterial activity of chitosan solution against Xanthomonas pathogenic bacteria isolated from Euphorbia pulcherrima,. Carbohydr Polym 72:287–292

50. Sawai J (2003) "Quantitative evaluation of antibacterial activities of metallic oxide powders (ZnO, MgO and CaO) by conductimetric assay,". J Microbiol Methods 54:177–182

Figures

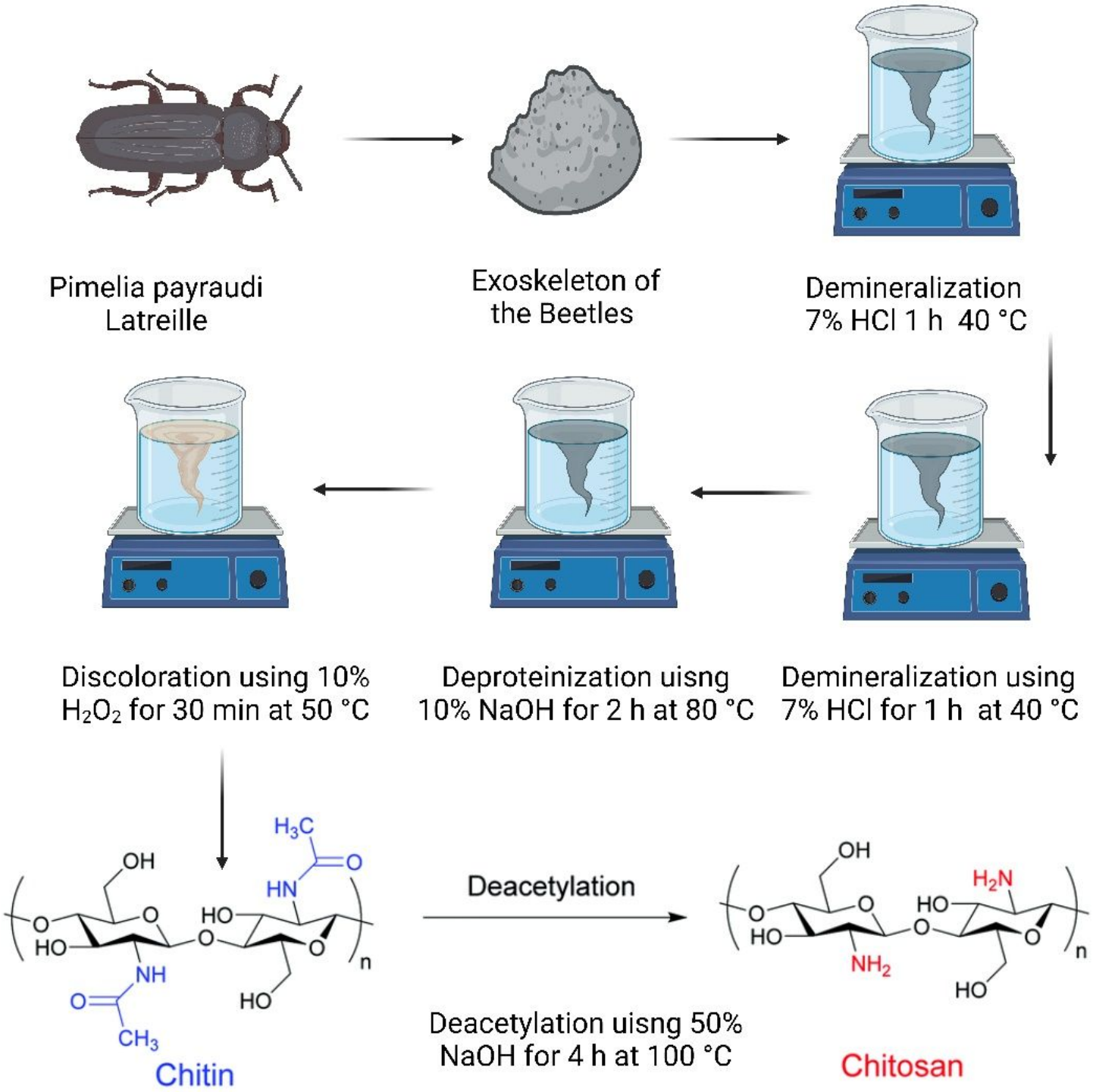

Figure 1

Schematic presentation showing extraction steps of chitosan from the exoskeletons of the beetle (Pimelia Payraudi Latreille).

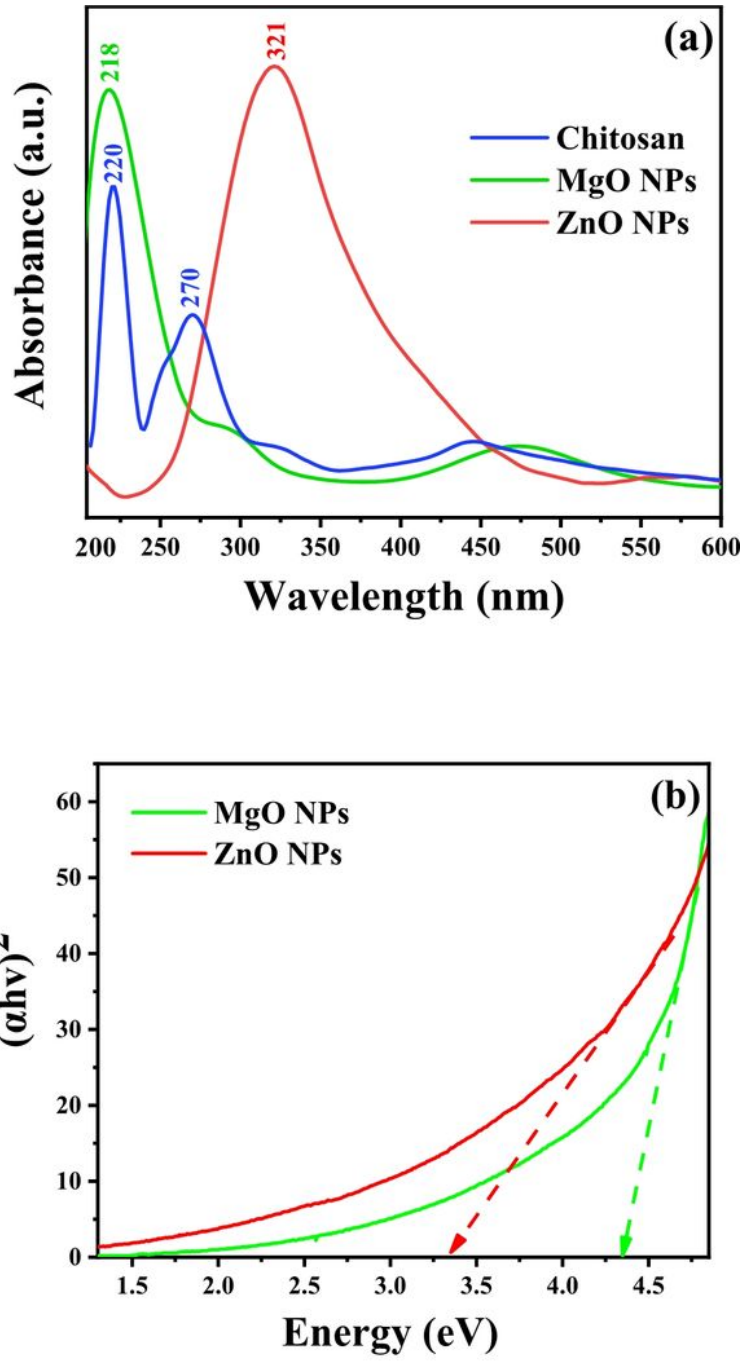

Figure 2

UV–Vis spectra of the chitosan from the exoskeletons of the beetle (Pimelia Payraudi Latreille), and the biosynthesized MgO NPs and ZnO NPs.

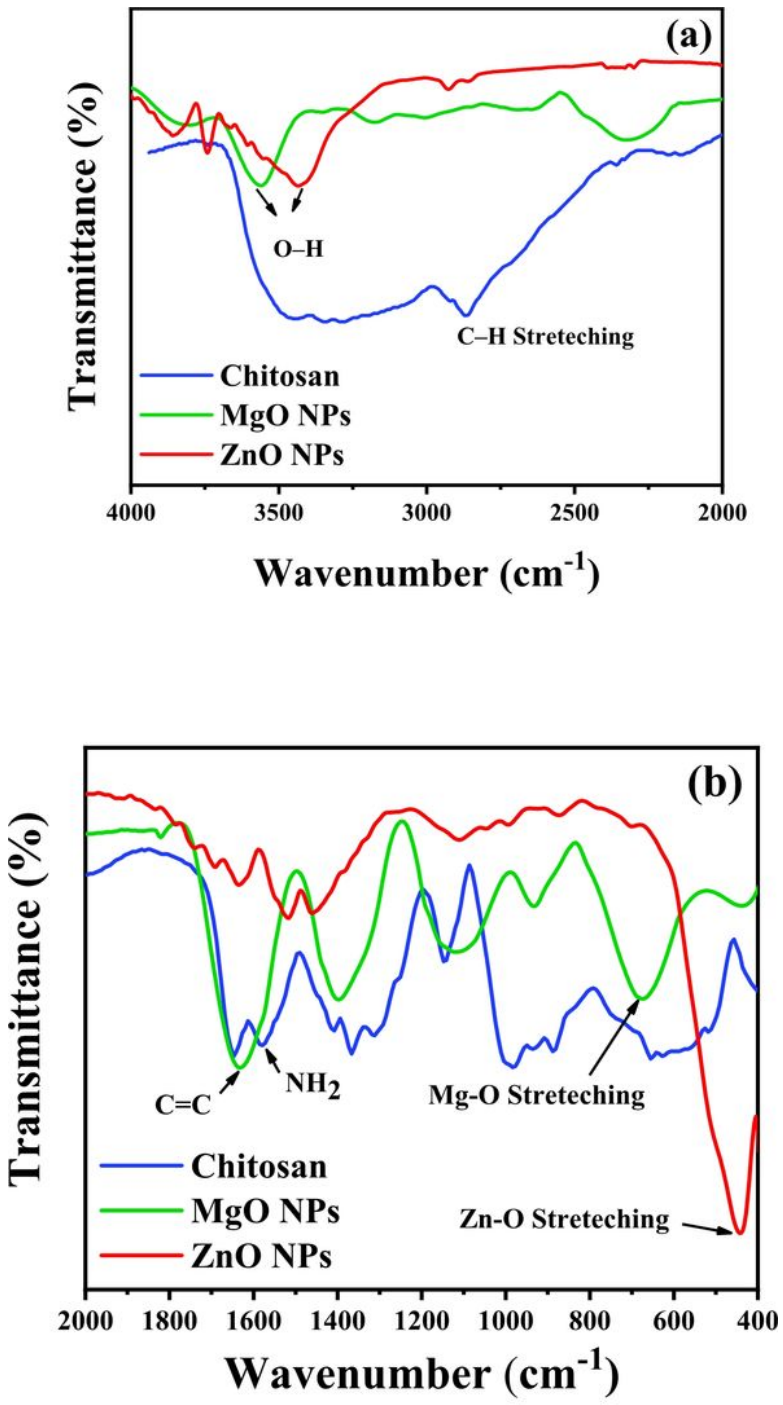

Figure 3

FTIR spectra of the chitosan from the exoskeletons of the beetle (Pimelia Payraudi Latreille), and the biosynthesized MgO NPs and ZnO NPs: (a) wavenumber between 2000-4000 cm-1and (b) wavenumber between 400-2000 cm-1.

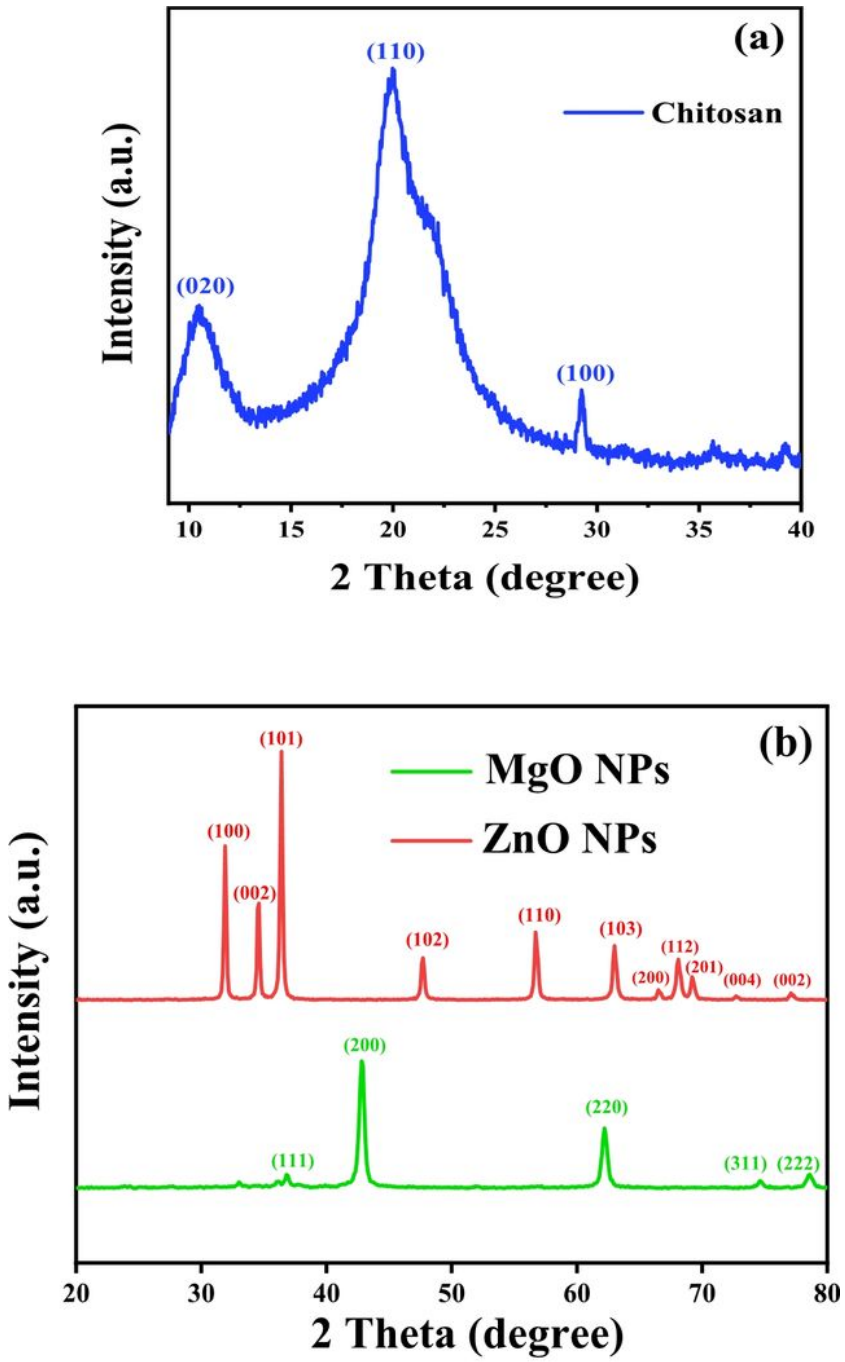

Figure 4

XRD diffraction pattern of (a) the chitosan from the exoskeletons of the beetle (Pimelia Payraudi Latreille), and (b) the biosynthesized MgO NPs and ZnO NPs.

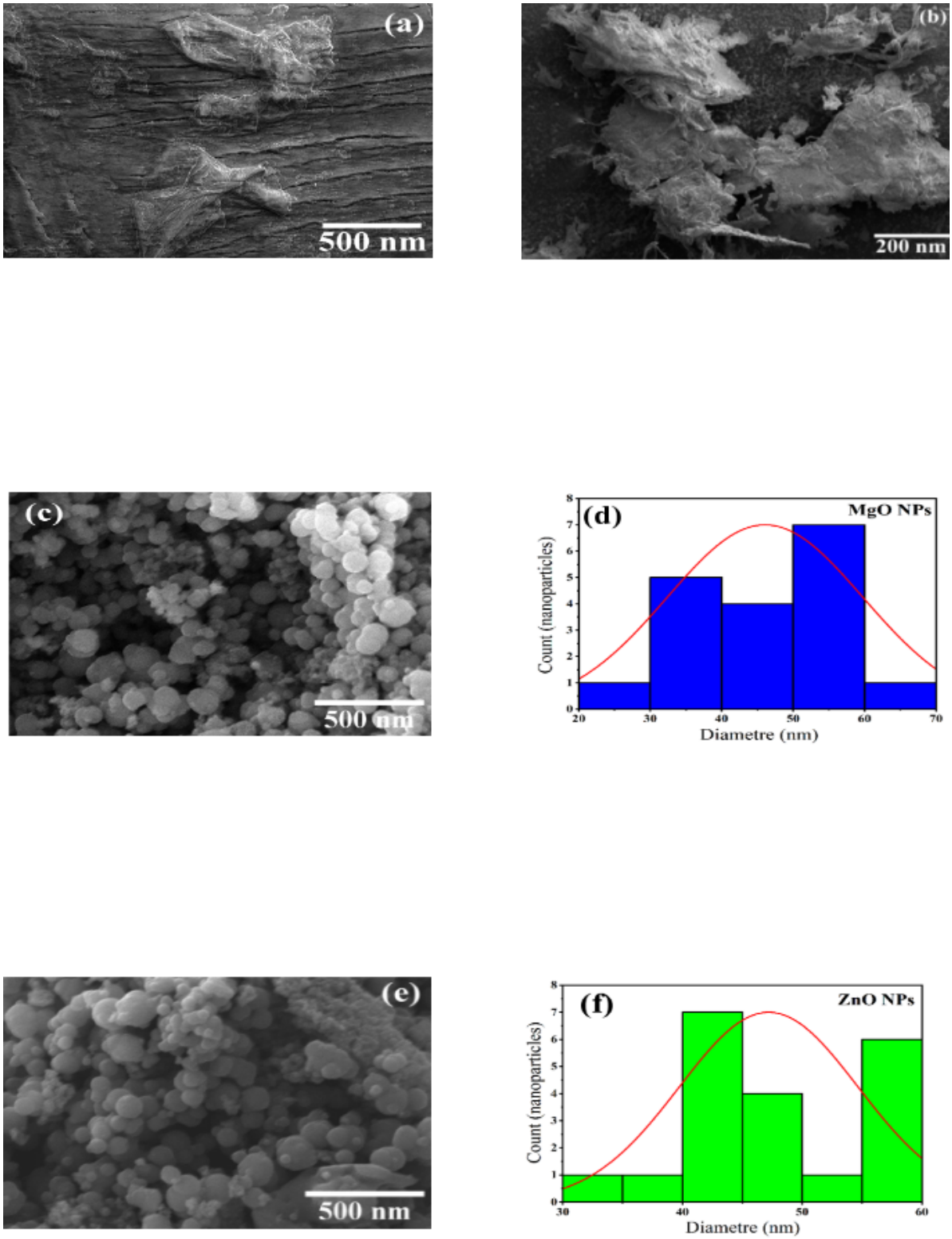

Figure 5

SEM analysis of the synthesized materials: (a,b) SEM image chitosan, (c,d) SEM image and particle size distributions of MgO NPs; (c,d) SEM image and particle size distributions of ZnO NPs; (g,h) SEM-EDX spectrum of MgO NPs and ZnO NPs, respectively.

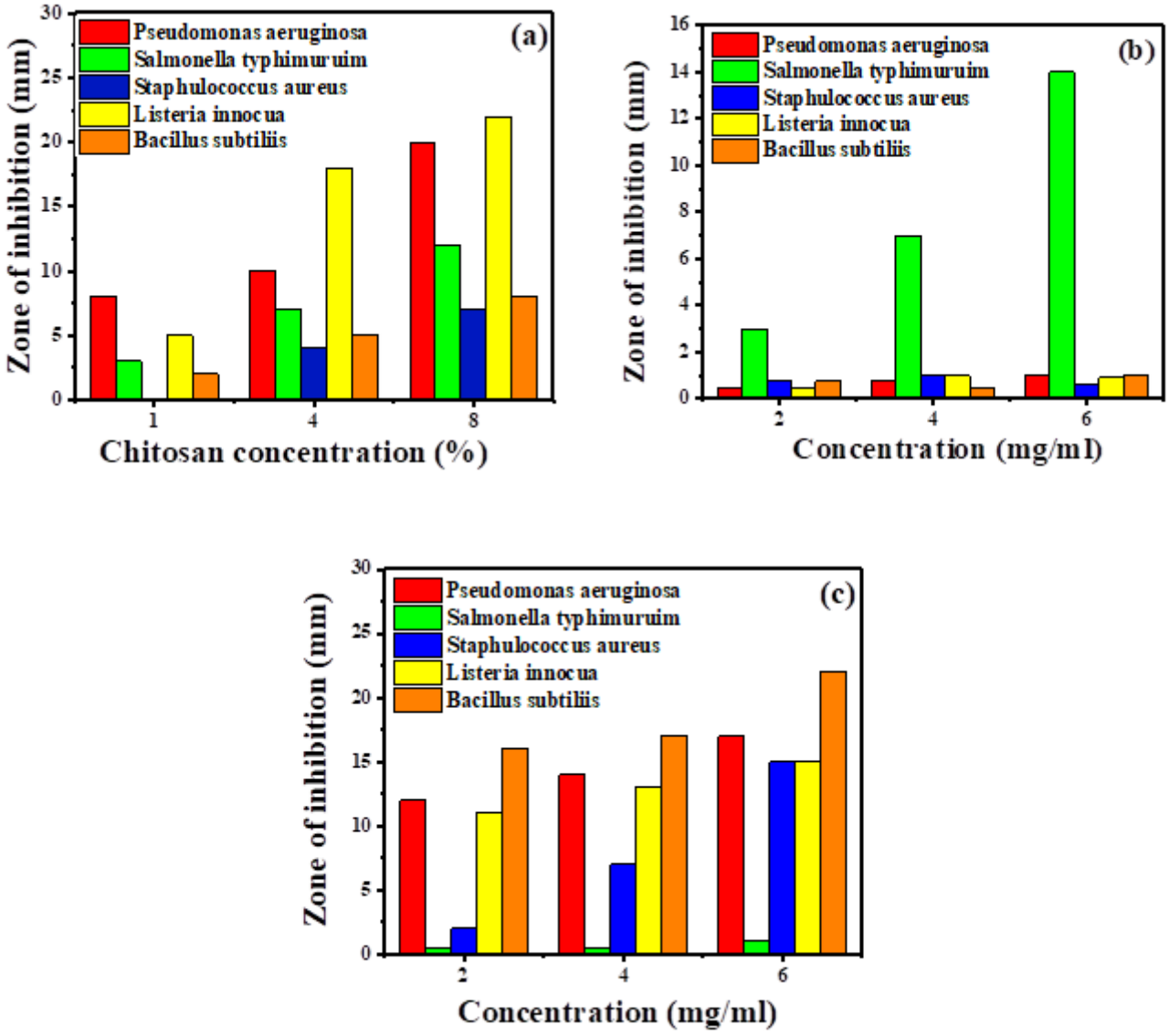

Figure 6

Antibacterial activity of (a) chitosan from the exoskeletons of the beetle (Pimelia Payraudi Latreille), (b) MgO NPs, and (c), ZnO NPs at various concentrations against different bacteria.

Supplementary Files

This is a list of supplementary files associated with this preprint. Click to download.

- floatimage1.jpeg